Evidence for a Narrow Anti-Charmed Baryon State

Jaroslav Cvach
on behalf of the H1 collaboration

Centre for Particle Physics, Institute of Physics AS CR, Na Slovance 2, 182 21 Prague 8)*

We report an observation of a narrow resonance state in $D^{*-}p$ and $D^{*+}\bar{p}$ in inelastic electron-proton collisions at centre-of-mass energies of 300 and 320 GeV at HERA. The resonance has a mass of 3099 $\pm$ 3 (stat.) $\pm$5 (syst.) MeV and width of 12 $\pm$ 3 (stat.) MeV, compatible with the experimental resolution. The resonance is interpreted as an anti-charmed baryon with a minimal constituent quark composition of $uudd\bar{c}$, together with the charge conjugate.

PACS: 13.60.-r, 14.20.Lq
Key words: Hadron spectroscopy, pentaquarks

1 Introduction

Several experiments have recently reported the observation of a narrow resonance with mass in the region of 1540 MeV, decaying to K^+n or K_s^0p [1]. If it is a particle it is a baryon with strangeness $S = +1$ charge +1 and baryon number $B = +1$. As it decays strongly it cannot consist of three constituent quarks as it must contain the anti-strange quark $\bar{s}$, and the $\bar{s}$ has negative baryon number. The possible quark configuration $uudd\bar{s}$ does not fit in the SU(3) classification scheme for strongly interacting particles (for critical review see e.g. [2]). Soon afterward, the NA49 collaboration from CERN reported not only this pentaquark state which has been named Θ^+ but evidence for a family of heavier particles close to the Θ^+ [3].

The H1 collaboration studied in detail the production of charmed and anti-charmed quarks in ep collisions where the dominant production mechanism is boson-gluon fusion, $\gamma^{(*)}g \rightarrow c\bar{c}$. The recent results cover the determination of the gluon density in the proton and measurement of the charm structure function F_2^c of the proton [4], the inclusive production of charmed mesons and diffractive production of J/ψ [5]. The large cross sections of charm production and good understanding of the detector turned the interest of the collaboration toward search for the production of pentaquarks with charm. The first evidence for a baryon with exotic quantum number in the charm sector has been recently reported [6] from this search. A resonance is observed when combining $D^{*-} \rightarrow \bar{D}^0\pi_s^- \rightarrow K^+\pi^-\pi_s^-$ candidates with proton candidates. A similar signal is seen in the charge conjugate mode and, therefore, in the remainder of the paper, particle charges are not generally given, unless it is explicitly stated [1])

*) This work is supported by Ministry of Education of the Czech Republic under the projects INGO-LA116/2000 and LN00A006.

[1]) The notation π_s is used to distinguish the low momentum pion released in the D^* decay from the D^0 decay.

2 Experimental Procedure

2.1 H1 apparatus

The tracks from charged particles are reconstructed in the H1 central tracker, whose main components are two cylindrical jet chambers (CJCs), covering the polar angle[2]) region $20^o < \theta < 160^o$. The information from the CJC sense wires is digitised using 100 MHz FADCs, providing simultaneous charge and timing information. The CJCs lie within a homogeneous magnetic field of 1.15 T, which allows measurements of the transverse momenta of charged particles. Two additional drift chambers complement the CJCs by precisely measuring the z coordinates of track segments. The Central Silicon Tracker is used to improve the charged track and event vertex reconstruction. The ionization energy loss of charged particles is derived from the mean of the inverse square-root of the charge collected by all CJC sense wires with a signal above threshold. The resolution of ionisation is $\simeq 8\%$ on average for minimum ionising particles.

A lead/scintillating fibre spaghetti calorimeter (SpaCal) contains both electromagnetic and hadronic sections. It is used to detect the scattered electron in deep inelastic scattering (DIS) events. The global characteristics of the hadronic final state are reconstructed using information from the central tracker, the SpaCal, and from a Liquid Argon Calorimeter, which surrounds the central tracker. The events are triggered on the basis of a scattered electron in the SpaCal, complemented by the signals in the CJCs and multi-wire proportional chambers in the central tracker. Further details of the H1 detector can be found in [7].

2.2 Data sample

The analysis is carried out using data taken in the years 1996-2000, when HERA collided electrons[3]) of energy 27.6 GeV with protons at 820 GeV (1997-1997) and 920 GeV (1998-2000). The integrated luminosity of the sample is 75 pb^{-1}. The selection of electron candidates was done in accordance to the standard H1 procedure for selection DIS events (see e. g. [8]). The virtuality of the exchanged photon lies in the range $1 < Q^2 < 100$ GeV^2 and the inelasticity of the event is required to satisfy $0.05 < y < 0.7$. This covers the region of effective measurement of the electron energy and angle in SpaCal and ensures that the hadronic final state lies in the central region of the detector. The DIS kinematic variables are defined as

$$Q^2 = -q^2, \quad y = q.p/k.p, \quad x = q^2/2q.p,$$

where q, k and p are the 4-vectors of the exchanged photon, the incident electron and the incident proton, respectively.

[2]) The positive z-axis is defined by the direction of the outgoing proton beam. The polar angle θ of a particle is defined relative to this axis and is related to the pseudorapidity η by $\eta = -\ln\tan\theta/2$.

[3]) The analysis uses data from periods when the beam lepton was either a positron (88% of the total) or an electron.

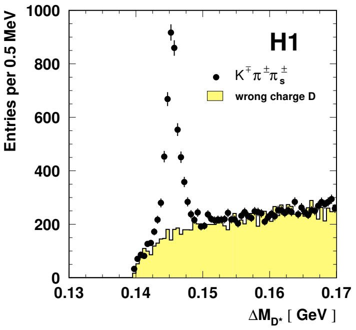

Fig. 1. ΔM_D^* distribution for $K^{\mp}\pi^{\pm}\pi_s^{\pm}$ combinations as described in the text. For comparison, the distribution from "wrong charge D" combinations, where the K and π yielding the D^0 mass have the same charge, is also shown.

D^0	$p_T(K) > 500$ MeV $p_T(\pi) > 250$ MeV $p_T(K) + p_T(\pi) > 2$ GeV $\lvert\Delta M_D^* - m(D^*) + m(D^0)\rvert < 2.5$ MeV
D^*	$p_T(\pi_s) > 120$ MeV $\lvert m(K\pi) - m(D^0)\rvert < 60$ MeV $p_T(D^*) > 1.5$ GeV $-1.5 < \eta(D^*) < 1$ $z(D^*) > 0.2$
p	$p_T(p) > 120$ MeV $L_p > 0.3$ for $p(p) < 2$ GeV $L_p > 0.1$ for $p(p) > 2$ GeV

Fig. 2. Summary of the kinematic and proton energy loss selection criteria applied to define D^* and proton candidates.

The decay channel $D^* \to D^0\pi_s \to K\pi\pi_s$ is used to reconstruct D^* mesons. The charged particle selection criteria, dE/dx requirements and transverse momentum cuts on the decay products are similar to those used in previous H1 analyses [4]. Unlike-charge particle combinations are made to form $K^{\mp}\pi^{\pm}$ pairs, where the particles are required to be consistent with kaons and pions according to their ionisation. Those combinations that give rise to an invariant mass within 60 MeV of nominal D^0 mass of 1864.5 MeV [9] are combined with a further pion candidate π_s with opposite charge to the kaon. The standard difference technique is used, based on the variable $\Delta M_D^* = m(K\pi\pi_s) - m(K\pi)$. A prominent signal is observed in the ΔM_D^* distribution (see Fig. 1) around the expected $D^* - D^0$ mass difference. The "wrong charge D" distribution is formed by $K^{\pm}\pi^{\pm}$ combinations in the accepted D^0 mass range. The "wrong charge D" distribution gives a good description of the correct-charge D^0 combinations away from the D^* peak. The kinematic cuts which were used to reduce the background to the D^* signal are summarised in the the first two rows in the Fig. 2, with the inelasticity $z(D^*) = (E - p_z)_{D^*}/2yE_e$, E_e being the electron beam energy.

Proton candidates are selected using requirements on the particle dE/dx measurements. The normalised proton likelihood L_p is defined to be the ratio of the proton likelihood to the sum of the pion, kaon and proton likelihoods[4]). The selection criteria for the proton candidate selection are given in the last row of the Fig. 2.

[4]) The likelihoods that a particle is a pion, kaon or proton are obtained from the proximity of the measured dE/dx to the most probable values for each particle type at the reconstructed momentum [10].

3 The Results

3.1 D^*p invariant mass distribution

The D^* and proton candidates are combined to form the mass difference $m(K\pi\pi_s p) - m(K\pi\pi_s)$, to which the D^* mass of 2010.0 MeV [9] is added to obtain the mass of the D^*p combination. The distribution are shown in Fig. 3 left for "opposite-charge" D^*p combinations ($K^-\pi^+\pi_s^+\bar{p}$ and $K^+\pi^-\pi_s^- p$) and in Fig. 3 right for

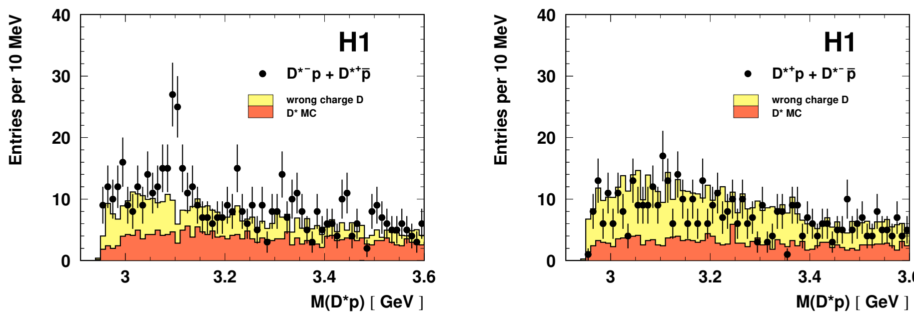

Fig. 3. Distribution in $M(D^*p)$ for opposite-charge (left) and same-charge (right) D^*p combinations. The data are compared with a two-component background model in which "wrong charge D" $K^\pm\pi^\pm$ combinations are used to describe non-charm related background and the D^* MC simulation describes background involving real D^* mesons.

"same-charge" D^*p combinations ($K^-\pi^+\pi_s^+ p$ and $K^+\pi^-\pi_s^-\bar{p}$). A clear and narrow peak is observed for the opposite-charge combinations at $M(D^*p) \simeq 3100$ MeV. Approximately half of the events in this signal arise from $D^{*-}p$ and from $D^{*+}\bar{p}$ combinations. The distribution for the same-charge combinations shows a small enhancement in the $M(D^*p)$ region in which the opposite-charge signal is observed.

The background distributions for the D^*p combinations are modeled by the sum of two contributions, which are shown in Fig. 3. Background from random combinations not involving charm is modeled using the "wrong charged D" combinations combined with proton candidates as for the correct-charge D^0 sample. Combinatorial background from D^* mesons with real or misidentified protons is modeled using simulated events from the RAPGAP [11] Monte Carlo model applied to D^* production in DIS, including string fragmentation and decays from JETSET [12]. The RAPGAP model gives a good description of the shapes of the inclusive D^* distributions.

An alternative model for the background distribution for the opposite-charge D^*p combinations - the DJANGO [13] - used for a simulation of both background components, gives similar distributions to those shown in Fig. 3. The same is true when the RAPGAP model of the D^*-related background is replaced by simulations with modified parton shower dynamics (CASCADE [14]) or fragmentation (HERWIG [15]). In all cases no resonant structures are observed in the simulated

$M(D^*p)$ distributions. The contribution from beauty decays have been considered using RAPGAP Monte Carlo simulation and found to be negligible.

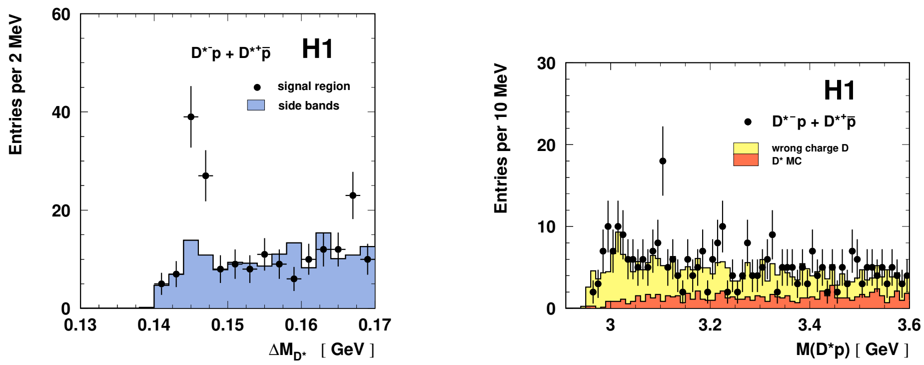

Fig. 4. (left) ΔM_D^* distribution for events in a 30 MeV window around the signal in the opposite-charge $M(D^*p)$ distribution, with no requirement on ΔM_D^*, compared with the corresponding distribution from side bands in the $M(D^*p)$ distribution, normalised according to the widths of the chosen sample regions.
(right) $M(D^*p)$ distribution for a low momentum proton selection with $p(p) < 1.2$ GeV. The data are compared with a two-component background model in which "wrong charge D" $K^\pm\pi^\pm$ combinations are used to describe non-charm related background and the D^* MC simulation describes background involving real D^* mesons.

The importance of the D^* and p content in the signal has been investigated in the following way. The ΔM_D^* distribution is shown in Fig. 4 left for events in a window $3085 < M(D^*p) < 3115$ MeV symmetrical around the D^*p signal. For comparison, a similar distribution is shown, taken from side bands with $2990 < M(D^*p) < 3070$ MeV and $3130 < M(D^*p) < 3210$ MeV, scaled by a factor 3/16 to account for the different interval widths. Away from the D^* peak the distribution in ΔM_D^* are similar. However, in the D^* meson region the distribution from the D^*p signal region clearly shows the significant excess of events well above those from the side bands. The signal region in $M(D^*p)$ is thus significantly richer in D^* mesons than the sideband.

The protons are clearly identified at low momentum. The analysis has been repeated with the proton momentum restricted to $p(p) < 1.2$ GeV, the measured $\mathrm{d}E/\mathrm{d}x$ required to be larger by a factor of at least 1.15 than that for a minimum ionizing particle and with the proton likelihood requirement increased to $L_p > 0.5$. With the tighter proton selection, the requirements on $z(D^*)$ and $p_T(K) + p_T(\pi)$ are removed. In Fig. 4 right, an enhancement in the $M(D^*p)$ distribution in the region of 3100 MeV is visible for this selection. The candidate tracks in the signal region $3085 < M(D^*p) < 3115$ MeV have an average $\langle L_p \rangle = 0.92$. No signal peaks are observed when the proton candidates are assumed to have the kaon or the pion mass. The signal is also not observed when the proton mass hypothesis is retained, but the $\mathrm{d}E/\mathrm{d}x$ requirement is modified to select pion or kaon candidates rather than proton candidates.

The analysis has also been done using an independent H1 data sample from photoproduction, where the scattered electron passes at a small angle into the backward beam pipe, implying $Q^2 < 1$ GeV^2. Again, a clear signal was observed near $M(D^*) = 3100$ MeV, with mass and width compatible with the DIS case.

3.2 Kinematic and reflection tests

Possible kinematic reflections that could fake the signal have been ruled out by studying invariant mass distributions and correlations involving the K, π, π_s and proton candidates under various particle mass hypotheses. For example, there is no evidence for any resonant structure or correlations with $M(D^*p)$ in the invariant mass combinations $m(Kp), m(\pi p), m(\pi_s p)$ of the proton candidates with the decay products of the D^* meson. Detailed studies have been carried out of the contribution to the $M(D^*p)$ distribution from $D_1^0(2420)$ and $D_2^{0*}(2460)$ mesons and their charge conjugates, both of which decay to $D^{*\pm}\pi^{\mp}$. The reflections due to both mesons when the decay pion is misidentified as a proton yield a broad distribution in $M(D^*p)$, with a maximum below the signal region. The predicted distribution within ± 24 MeV of the observed peak is approximately four events. The signal in the measured $M(D^*p)$ distribution covers the full available phase space in $M(D^*\pi)$, with no evidence for enhancements in the region of the D_1^0 and D_2^{0*} mesons.

The kinematics of the D^* and proton candidates from the decay of a resonance would be expected to be harder than those of the background distribution. Two side bands with larger and smaller $M(D^*p)$ than the signal give rise to compatible proton momentum spectra, both of which are significantly softer than that in the signal region. If the $M(D^*p)$ distribution is plotted for $p(p) > 2$ GeV with no requirement on the proton likelihood, a strong signal is observed, with a reduced background. The peak value and width of the signal are compatible with those for the standard selection shown in Fig. 3.

4 Signal assessment

Fits to the $M(D^*p)$ distribution from the opposite-charge D^*p combinations have been carried out to evaluate the peak position, width and statistical significance. Assuming the measured width to be dominated by the experimental resolution, a Gaussian distribution is used for the signal, with the peak position, the width and the normalisation as free parameters. The results of the fit for the $D^{*-}p + D^{*+}\bar{p}$ combinations are compared with the data in Fig. 5. The fit yields the following values

$$M_{peak} = 3099 \pm 3 \text{ MeV}, \quad \Gamma_{peak} = 12 \pm 3 \text{ MeV}, \quad N_s = 50.6 \pm 11.2$$

where N_s is the number of events in the signal. The observed resonance is estimated to contribute roughly 1% of the total D^* production rate. The Gaussian width of the signal is compatible with the experimental resolution of 7 ± 2 MeV. The fit repeated separately for each charge mode $D^{*-}p$ and $D^{*+}\bar{p}$ gives values of M_{peak} and

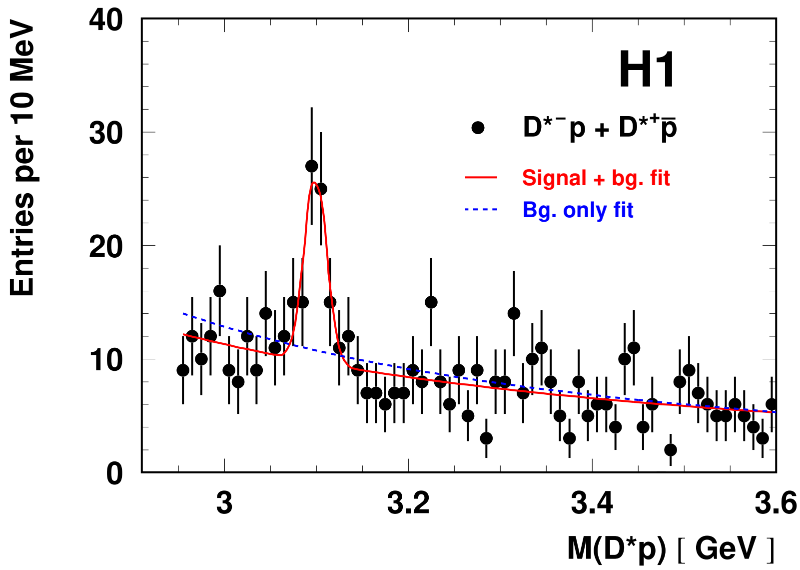

Fig. 5. ΔM_D^* distribution from the opposite-charge D^*p combinations compared with the results of a fit in which both signal and background components are included (solid line) and with the results of a fit in which only the background component is included (dashed line).

of Γ_{peak} compatible within errors with those of the full sample. Also within errors, the number of events in the signal N_s does not depend on the charge combination. The fit results are not significantly affected by another background parametrisation, shifts in the binning and changes to the bin width in the range 1 MeV to 20 MeV. The systematic uncertainty on the mass of the peak is 5 MeV.

The probability that the background distribution fluctuates to produce the signal has been evaluated by comparing the observed number of events with background estimates for a window corresponding to $\pm 2\sigma$ around the peak position according to the fit. The total number of events in this interval is 95. We used a more conservative background estimate and fitted the power-law function to the full $M(D^*p)$ distribution (see Fig. 5 - dashed line). The corresponding background estimate is $N_b = 51.7 \pm 2.7$ (stat.) [5]). The probability that a background of $N_b = 51.7$ fluctuates to produce at least the number of events in the signal is 4.10^{-8}, assuming Poisson statistics. This probability corresponds to 5.4σ when expressed as an

[5]) The background contribution estimated using the fit with signal (full line in Fig. 5) is $N_b = 45.0 \pm 2.8$ (stat.).

equivalent number of Gaussian standard deviations.

5 Summary

A clear and narrow resonance is observed for both $D^{*-}p$ and $D^{*+}\bar{p}$ combinations with an invariant mass of $M(D^{*}p) = 3099 \pm 3$ (stat.) ± 3 (stat.) ± 5 (syst.) MeV in H1 deep inelastic electron-proton scattering data.v The probability for the background distribution to fluctuate to produce a signal as large as that observed is 4.10^{-8}. The measured RMS width of the resonance is 12 ± 3 (stat.) MeV, consistent with the experimental resolution. The resonance is interpreted as an anti-charmed baryon decaying to $D^{*-}p$ and its charge conjugate decaying into $D^{*+}\bar{p}$. The minimal constituent quark composition of such a baryon is $uudd\bar{c}$, making it a candidate for a charmed pentaquark state.

I am indebted to all members of the H1 collaboration who contributed to the result. Especially, I would like to thank to K. Daum and K. Lipka for providing me with the material for the talk and M. Bednář, J. Gayler, T. Greenshaw and V. Chekelyan for help with the text of the contribution.

References

[1] see talk of M. Karliner at this conference.

[2] N. P. Samlos, M. Goldberg, B. T. Meadows: Rev. Mod. Phys. **46** (1974) 49.

[3] see talk of D. Barna at this conference.

[4] C. Adloff et al.: Nucl. Phys. **B545** (1999) 21, hep-ex/9812023;
C. Adloff et al.: Phys. Lett. **B528** (2002) 119, hep-ex/0108039.

[5] A. Aktas et al.: preprint DESY-04-156, Eur. Phys. J. (in press), hep-ex/0408146;
A. Aktas et al.: Phys. Lett. **B568** (2003) 205, hep-ex/0306013.

[6] A. Aktas et al.: Eur. J. Phys. **B588** (2004) 17, hep-ex/0403017.

[7] I. Abt et al.: Nucl. Inst. Meth. **A386** (1997) 310 and 348.

[8] C. Adloff et al:, Eur. Phys. J. **C21** (2001) 33, hep-ex/0012053.

[9] Particle Data group, H. Hagiwara et al.: Phys. Rev. **D66** (2002) 199.

[10] J. Steinhart, PhD thesis, Universität Hamburg, Germany, 1999.

[11] H. Jung, Comp. Phys. Commun. **86** (1995) 147.

[12] B. Anderson, G. Gustafson, G. Ingelman and T. Sjöstrand, Phys. Rep. **97** (1983) 31.

[13] A. Kwiatkowski, H. Spiesberger and H. J. Möhring, Comp. Phys. Commun. **69** (1992) 155:
L. Lönnbland, Comp. Phys. Commun. **71** (1992) 15.

[14] H. Jung and G. P. Salam, Eur. Phys. J. **C19** (2001) 351.

[15] G. Marchessini et al.: Comp. Phys. Commun. **67** (1992) 465.